Synthesis and Characterization of Two Lanthanide (Gd3+ and Dy3+)-Based Three-Dimensional Metal Organic Frameworks with Squashed Metallomacrocycle Type Building Blocks and Their Mag...

ARTICLE *in* CRYSTAL GROWTH & DESIGN · FEBRUARY 2014

Impact Factor: 4.89 · DOI: 10.1021/cg401804e

5 AUTHORS, INCLUDING:

Soumava Biswas
Indian Institute of Science Education and Res...
17 PUBLICATIONS **177** CITATIONS
SEE PROFILE

Himanshu Sekhar Jena
Osaka University
36 PUBLICATIONS **289** CITATIONS
SEE PROFILE

Soumyabrata Goswami
Indian Institute of Science Education and Res...
22 PUBLICATIONS **161** CITATIONS
SEE PROFILE

Sanda Suresh
Indian Institute of Science Education and Res...
17 PUBLICATIONS **135** CITATIONS
SEE PROFILE

CRYSTAL GROWTH & DESIGN

Article

pubs.acs.org/crystal

Synthesis and Characterization of Two Lanthanide (Gd^{3+} and Dy^{3+})-Based Three-Dimensional Metal Organic Frameworks with Squashed Metallomacrocycle Type Building Blocks and Their Magnetic, Sorption, and Fluorescence Properties Study

Soumava Biswas, Himanshu Sekhar Jena, Soumyabrata Goswami, Suresh Sanda, and Sanjit Konar*

Department of Chemistry, IISER Bhopal, Bhopal-462066, India

Supporting Information

ABSTRACT: Two novel isostructural lanthanide- based three-dimensional (3D) metal organic frameworks (MOFs), $[Ln_2(pam)_3(DMF)_2(H_2O)_2]_n \cdot n$DMF {Ln = Gd(**1**), Dy(**2**); H_2pam = 4,4′-methylenebis[3-hydroxy-2-naphthalenecarboxylic acid]} using the pharmaceutical agent "pamoic acid (H_2pam)" are synthesized for the first time. Single crystal structure analysis shows that the 3D framework originates from the self-assembly of lanthanide metallomacrocycles made of dumble-shaped basic secondary building units and having channels of sizes 17.427 × 15.163 Å (for **1**) and 14.58 × 17.23 Å (for **2**), respectively. In both the complexes, two eight-coordinated lanthanide centers are connected with six pamoate groups to give a paddle-wheel type building block. The arrangement of pamoates and lanthanides in the framework provokes both right- (*P*) and left-hand (*M*) helicity around the 2_1 screw axis. The magnetic measurements show that complex **1** acts as a cryogenic magnetic refrigerant having magnetic entropy change, $-\Delta S_m$, of 17.25 J kg^{-1} K^{-1}(ΔH = 7 T at 3 K), and complex **2** shows slow relaxation of magnetization. The adsorption studies reveal that complexes **1** and **2** show selectivity toward CO_2 sorption over other gases and exhibit high methanol vapor uptake (227 cm^3 g^{-1} for **1** and 201 cm^3 g^{-1} for **2**). Solid state photoluminescence properties reveal that they are photoluminescent materials.

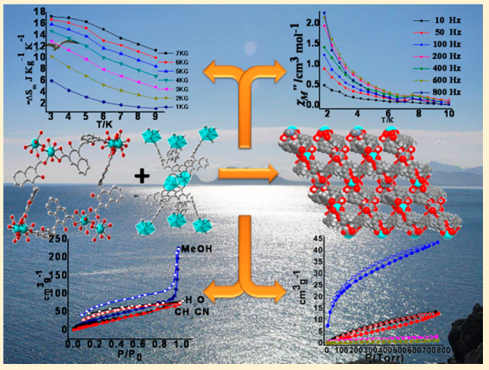

INTRODUCTION

Metal−organic frameworks (MOFs) are intriguing classes of materials that have attracted intense research attention due to their versatile structural features, such as high surface area,[1] uniform cavities with predesigned molecular dimensions, tunable pore size, and pore functionalization,[2] making them very auspicious for a wide range of applications in a variety of areas like gas storage, separation, proton conductivity, controlled drug delivery, etc.[3] An enormous amount of work has been done in this area by scientists like Kitagawa,[4] Yaghi,[5] Ferey,[6] Hupp,[7,1d] Cooper,[8] Rosseinsky,[9] Zhou,[10] Clearfield,[11] Chupas[12] and several others.[13] In terms of application, one limitation of MOF is that most of the properties are related to pore size and surface area of the network. As the adsorption capability of MOFs are expressed by weight percentage, scientists are looking for more and more lighter metals like lithium. The metal centers which are used as nodes for constructing the framework play a secondary role. Lanthanide (Ln)-containing MOFs have attracted interest partly due to the metal itself, as they are able to incorporate both photoluminescent centers and magnetic properties in addition to the other properties related to pore size and surface area.[14−16] The feature makes them ideal for developing new multifunctional materials.

Peng et al. have reported different multifunctional lanthanide MOFs with different dicarboxylates having C_2 symmetry. They substantiate that the selection of organic ligands with special symmetry not only is crucial to overcome the difficulty in synthesizing lanthanide three-dimensional (3D) MOFs but also could be a good material to explore their sorption behaviors along with other properties.[17] On the contrary, Ln-framework made of pharmaceutical ingredients "pamoic acid (H_2pam) or embonic acid" are not known so far, although a limited number of its transition metal complexes are reported.[18]

In this contribution, two isostructural lanthanide-based 3D MOFs, $[Ln_2(pam)_3(DMF)_2(H_2O)_2]\cdot n$DMF [Ln = Gd^{3+} (**1**), and Dy^{3+} (**2**)] were synthesized and structurally characterized. The magnetic characterization reveals that complex **1** shows cryogenic magnetic refrigeration properties, whereas **2** shows slow relaxation of magnetization. Complexes **1** and **2** exhibit high methanol vapor uptake and selectivity toward CO_2 sorption over other gases. The ligand pamoic acid provides good metal-to-metal distance for large pore size and also behaves like a suitable chromophoric moiety(antena) for

Received: December 3, 2013
Revised: January 21, 2014
Published: February 3, 2014

   dx.doi.org/10.1021/cg401804e | *Cryst. Growth Des.* 2014, 14, 1287−1295

sensitization of the lanthanides, and that has been revealed by its photophysical properties.

EXPERIMENTAL SECTION

Materials and General Procedure. All the reagents and solvents were commercially available and were used as obtained. Pamoic acid, $Gd(NO_3)_3{\cdot}6H_2O$, and $Dy(NO_3)_3{\cdot}6H_2O$ were obtained from the Sigma Aldrich Chemical Company and used as received.

The elemental analyses were carried out on Elementar Micro vario Cube elemental analyzer. FT-IR spectra (4000−400 cm^{-1}) were recorded on KBr pellets with a Perkin-Elmer Spectrum BX spectrometer. Cary Eclipse EL05033882 was used for fluorescence spectra. Powder X-ray diffraction (PXRD) data were collected on a PANalytical EMPYREAN instrument, using Cu Kα radiation. In order to evaluate the porous property of both complexes, the crystalline materials are grounded to powder and activated by drying under vacuum at 100 °C for 10 h. Gas and solvent vapor adsorption studies were performed using a BELSORP MAX (BEL JAPAN) volumetric adsorption analyzer. Magnetic measurements were performed using a Quantum Design SQUID VSM magnetometer. The measured values were corrected for the experimentally measured contribution of the sample holder, while the derived susceptibilities were corrected for the diamagnetism of the samples, estimated from Pascal's tables.[19]

Crystal Data Collection and Structure Determination. Suitable single crystals of each of the complexes were mounted on a Bruker SMART diffractometer equipped with a graphite monochromator and Mo Kα (λ = 0.71073 Å, 140 K) radiation. Data collection was performed using ϕ and ω scans. The structures were solved using direct methods followed by full matrix least-squares refinements against F^2 (all data HKLF 4 format) using SHELXTL.[20] Subsequent difference Fourier synthesis and least-squares refinement revealed the positions of the remaining nonhydrogen atoms. Determinations of the crystal system, orientation matrix, and cell dimensions were performed according to the established procedures. Lorentz polarization and multiscan absorption correction were applied. Nonhydrogen atoms were refined with independent anisotropic displacement parameters, and hydrogen atoms were placed geometrically and refined using the riding model. All calculations were carried out using SHELXL 97,[21] PLATON 99,[22] and WinGX system, version 1.64.[23] The solvent DMF molecules in **1** and **2** are highly disordered, and attempts to locate H atoms on the calculated positions by riding method (for **1**) were unsuccessful, which results in a larger Hirschfield difference for N1−C38 and C36. Similarly, in **2**, the DMF (C36, C38, and N1) molecules are disorderd. Since both the complexes show solvent accessible voids, SQUEEZE[23] was used, and a new .HKL file was generated. The structure was solved by using the newly generated .HKL file. Structure refinement after modification of the data with the SQUEEZE routine led to better refinement and data convergence. Detailed instruction from the .SQF file is included in the final .cif file. From the TG analysis, it is confirmed that only one noncoordinated DMF molecule are present, which is removed by the SQUEEZE program and, hence, included in the molecular formula. Data collection and structure refinement parameters and crystallographic data for the two complexes are given in Table 1.

Synthesis of $[Gd_2(pam)_3(DMF)_2(H_2O)_2]_n{\cdot}nDMF$ (1). To a 10 mL solution of methanol and DMF (1:1), $Gd(NO_3)_3{\cdot}6H_2O$ (0.2 mmol, 90 mg) was added, and the solution was stirred for 10 min to dissolve completely. To this solution, pamoic acid (0.3 mmol, 116.5 mg) was added part-by-part, and stirring of the solution continued. After 15 min, 2 drops of pyridine were added and allowed to stir for 1 h more. The solution was then filtered, and the filtrate was kept for crystallization at room temperature. After one day, pale yellow single crystals were separated by filtration, washed with DMF, and dried in air. Yield: 170 mg (52%). Elemental analysis (%): Calcd (found) for $C_{78}H_{67}Gd_2N_3O_{23}$: C, 54.19(53.84); H, 3.91(3.45); N, 2.43(2.13). Selected IR data (4000−400 cm^{-1}, KBr pellet): 3412(b), 1648(s), 1546(m), 1399(s), 1349(m), 1329(w), 1303(w), 1029(s), 912(w), 812(s), 749(s), 601(s), 437(w).

Table 1. Summary of X-ray Crystallographic Data for 1 and 2[a]

	1	2
CCDC number	941734	942172
formula	$C_{78}H_{67}Gd_2N_3O_{23}$	$C_{78}H_{67}Dy_2N_3O_{23}$
formula mass	1728.87	1739.37
wavelength (Å)	0.71073	0.71073
temperature (K)	140	140
crystal system	monoclinic	monoclinic
space group	$C2/c$	$C2/c$
a (Å)	31.517(12)	31.28(3)
b (Å)	14.882(4)	14.735(13)
c (Å)	28.494(8)	28.51(5)
α (deg)	90.00	90.00
β (deg)	120.19(2)	120.13(5)
γ (deg)	90.00	90.00
V (Å^3)	11552(6)	11365(24)
Z	4	4
D ($_C$/g^{-3})	0.942	0.972
μ (Mo Kα) (cm^{-1})	1.186	1.353
F(000)	3240	3312
reflection	13267	13215
unique	13041	9604
GOOF on F^2	1.171	1.251
$R1^a$ [$I > 2\sigma I$]	0.0623	0.0737
$wR2^b$ [$I > 2\sigma I$]	0.1532	0.1251
$(\Delta\rho)_{max}$, $(\Delta\rho)_{min}$ (e A^{-3})	1.023, −1.007	1.131, −1.321

[a] $R1 = \Sigma||F_o| - |F_c||/\Sigma|F_o|$ and $wR2 = |\Sigma w(|F_o|^2 - |F_c|^2)|/\Sigma|w(F_o)^2|^{1/2}$.

Synthesis of $[Dy_2(pam)_3(DMF)_2(H_2O)_2]_n{\cdot}nDMF$ (2). Complex **2** was prepared following the same procedure used for **1**, using $Dy(NO_3)_3{\cdot}6H_2O$ (0.2 mmol, 91 mg) instead of $Gd(NO_3)_3{\cdot}6H_2O$. After one day, pale yellow single crystals were separated by filtration, washed with DMF, and dried in air. Yield: 162 mg (49%). Elemental analysis (%): Calcd (found) for $C_{78}H_{67}Dy_2N_3O_{23}$: C, 53.86(53.32); H, 3.88(3.57); N, 2.42(2.16). Selected IR data (4000−400 cm^{-1}, KBr pellet): 3415(b), 1642(s), 1383(s), 1346(m), 1327(w), 1300(w), 1237(s), 1204(s), 1153(w), 1094(s), 957(m), 880(m), 758(s), 680(w), 601(s), 439(w).

RESULTS AND DISCUSSIONS

We used pamoic acid as building blocks for several reasons: (1) it exhibits a long distance between two coordination points of the carboxylate group, which makes it convenient to act as a spacer in building a porous network; (2) it possesses both rigidity from the naphthyl rings and flexibility from the twisted C−CH_2−C single bond, which could lead to a possible helical architecture; (3) it exhibits delicate $\pi-\pi$ stacking interactions, which often plays a decisive role in regulating supramolecular networks; and (4) its metal complexes can be used as electrical conductors as well as potential fluorescent materials.[24] During synthesis of **1** and **2**, few drops of pyridine have been added to facilitate deprotonation of pamoic acid. Although triethylamine does the same job, the crystals isolated using pyridine are of better diffracting qualities than that of triethylamine. The absence of characteristic absorption of ν_{as}(COOH) near 1700 cm^{-1} indicates that pamoic acid is completely deprotoned in both complexes. The $\nu_{as}(COO^-)$ vibration of the carboxylate group occurs at 1648 and 1642 cm^{-1} for **1** and **2**, respectively, while those of $\nu_s(COO^-)$ occur at 1399 and 1383 cm^{-1}, respectively. The large difference in the $\Delta(\nu_{as}-\nu_s)$ values of 249−300 cm^{-1} for **1** and 243−310 cm^{-1} for **2** evidence the presence of both chelating bidentate and bis-monodentate

dx.doi.org/10.1021/cg401804e | Cryst. Growth Des. 2014, 14, 1287−1295

mode of pamoates (Scheme S1 of the Supporting Information).[25] TG analysis (Figure S1 of the Supporting Information) shows a weight loss of ~5% (calculated ~4%) in the temperature range of 120−160 °C, which might be due to the loss of one noncoordinated DMF molecule from the framework. The desolvated framework displays a weight loss of ~10% (calculated ~10%) in the temperature range of 180−290 °C, which corresponds to the loss of two coordinated water and two DMF molecules from the frameworks. The bulk phase powder X-ray diffraction patterns of both complexes is in good agreement with the simulated one based on the single crystal structure data (Figure S2 of the Supporting Information), indicating the purity of the as-synthesized product.

Structural Description for Complexes 1(Gd) and 2(Dy). Single-crystal X-ray diffraction analysis reveals that complexes **1** and **2** are isostructural in nature and crystallize in the monoclinic space group *C*2/*c*. As illustrated in Figure S3(a) of the Supporting Information, the asymmetric unit contains similar core structure $[Ln(pam)_{1.5}(DMF)(H_2O)]$ [where Ln = Gd(**1**) and Dy(**2**)] having one Ln ion, one and half of pamoate ligands, one DMF, and one coordinated water molecule. In both complexes, each Ln centers are eight-coordinated with six oxygen atoms from two pamoate ligands, one oxygen atom from the DMF molecule, and one coordinated water molecule. Thus the coordination arrangement around the Ln centers can be described as a distorted square antiprismatic (Figure S3(b) of the Supporting Information). The Ln−O bond lengths are in the range of 2.297(4)− 2.458(5) Å for **1** and of 2.306(6)−2.48(1) Å for **2**, respectively. The relevant bond parameters around the Ln centers are listed in Table S1 of the Supporting Information. In both complexes, the flexible skeleton of pam^{2-} is twisted, and the hydroxy and carboxyl groups adopt an anti (staggered) conformation to minimize the steric hindrance. In addition, intramolecular H-bonding interactions between them further stabilize the conformation. The H-bond parameters are listed in Table S2 of the Supporting Information. The dihedral angles between two naphthyl moieties of two pamoate ligands in **1** and **2** are different and were found to be 77.77° and 82.44° and 77.19° and 79.73°, respectively.

It is important to note that in both complexes, two pamoate ligands uniquely adopt two different bridging modes (Figure 1 and Scheme S1 of the Supporting Information) [i.e., one is in both the monodentate and the chelating bidentate mode (type I, left) and the other is in only the monodentate bridging mode (type II, right) and can be viewed as μ_3- and μ_4-connectors, respectively, to form a 2D framework having a channel of size 17.427 × 15.163 Å (for **1**) and 14.58 × 17.23 Å (for **2**), as shown in Figure S4 of the Supporting Information]. Although the channel size has been calculated taking Ln···Ln and CH_2···CH_2 separations into consideration, the real volume of the cavities are further reduced due to the significant offset stacking of naphthyl moieties of pamoate inside the framework. The two types of pamoates are arranged alternatively in the framework (Figure S5 of the Supporting Information), where the lanthanides are arranged like "tiles" on the floor (Figures S6 and S7 of the Supporting Information).

In overall, it can be seen that the noted extended two-dimensional (2D) framework is formed by squashed metallomacrocycles (Figure 2), originating from the basic secondary building units (SBU) $[Ln_2(pam)_6(DMF)_2(H_2O)_2]$, as shown in Figure S8 of the Supporting Information. Also, each SBU is connected to six nearby SBUs through pamoate ligands. Overall, its representation is similar to a dumble [Figure 3 (left)], and its schematic representation is illustrated in Figure 3 (right).

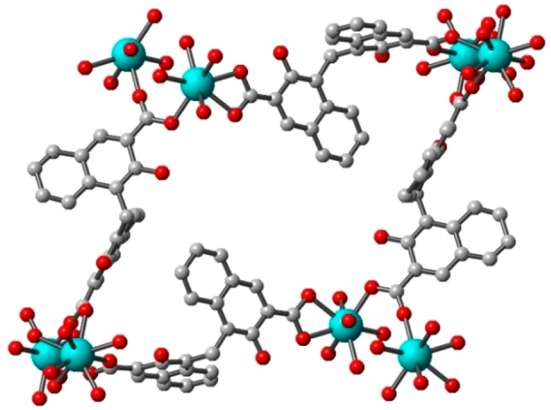

Figure 2. Illustration of lanthanide metallomacrocycle found in **1**.

In the SBU, two types of pamoate ligands are coordinated to lanthanide dimers (i.e., two type I and four type II). The Ln···Ln distances in the unit are 4.229(1) Å for **1** and 4.214(3) Å for **2**, respectively. The oxygen atoms of type II pamoates bridge the lanthanide centers symmetrically, which results in a very rare lanthanide paddle wheel structure [Figure S9(a) of the

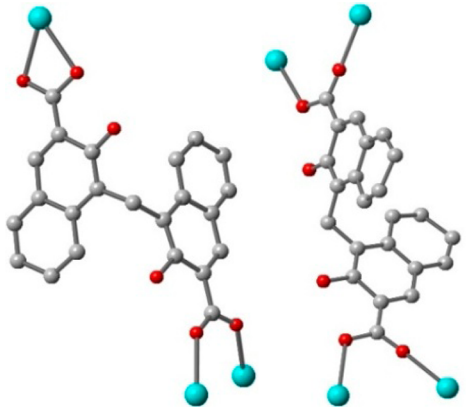

Figure 1. Illustration of two types of bridging mode of pamoic acid type I (left) and type II (right) observed in complexes **1** and **2**.

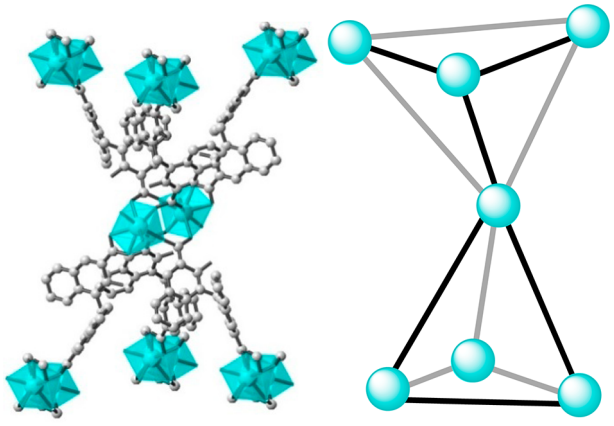

Figure 3. Views representing the connection of each SBU to six nearby SBUs though pamoate ligands, overall showing a dumble shape (left) and its schematic view (right).

dx.doi.org/10.1021/cg401804e | *Cryst. Growth Des.* 2014, 14, 1287−1295

Supporting Information][27] where pamoates form a dihedral angle of 86.99°(**1**) and 88.97°(**2**), respectively. Each lanthanide paddle wheel connected to six nearby units through the six pamoate groups and extended in one-dimensional (1D) fashion, as shown in Figure S9(b) of the Supporting Information. For both complexes, the Ln···Ln separations between the paddle wheels (between the SBUs) are ∼15 Å. Viewing the lattice of **1** along the *c* axis illustrates helical arrangement of lanthanide pamoates [right (*P*) and left-handed (*M*)], which further extended to a 2D array by another V-shaped pamoate, as shown in Figure 4. The helix generated

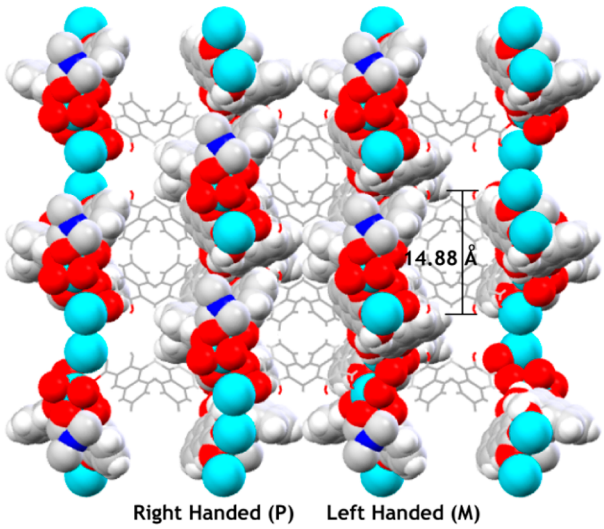

Figure 4. Illustration of helical chain [right (P) and left-handed (M)] found in complex **1**.

around the 2_1 screw axis exhibit a pitch of 14.88 Å (for **1**) and 14.70 Å (for **2**), respectively. Here it is very important to note that in the framework, the usual $\pi\cdots\pi$ interactions between naphthyl moieties are affected by the intervening of another naphthyl moiety in between them. Moreover, in the 3D framework (Figure S10 of the Supporting Information), the SBUs are organized through different noncovalent interactions, such as edge-to-face C−H···π and C−H···O interactions and the naphthyl moieties are slipped over one another, having a cg···cg distance of 5.316 Å. PLATON analysis[26] revealed a pore-accessible volume of 53.9%, with respect to the whole unit cell volume (6226.5 Å^3 out of the 11552.0 Å^3 per unit cell volume) for complex **1** and 50.7% with respect to the whole unit cell volume (5766.2 Å^3 out of the 11365.0 Å^3 per unit cell volume) for complex **2**, respectively.

Magnetic Property Studies. The bulk purity of both complexes **1** and **2** were confirmed by comparing the corresponding simulated and experimental PXRD patterns (Figure S2 of the Supporting Information). The DC magnetic susceptibility data for **1** and **2** were collected in the temperature range of 1.8−300 K at 1KG (Figures 5 and 6). The room temperature $\chi_M T$ (χ_M = molar magnetic susceptibility) value was found to be 15.36 cm^3 mol^{-1} K for **1** (calculated $\chi_M T$ = 15.6 cm^3 mol^{-1} K for two noninteracting Gd^{3+}on ($^8S_{7/2}$, g = 1.99). The small difference between the calculated and experimental $\chi_M T$ value is due to the antiferromagnetic coupling between the Gd^{3+} centers. Upon cooling, this value remains almost constant up to 30 K and decreases down to reach a value of 14.11 cm^3 mol^{-1} K at 1.9 K. The shape of the

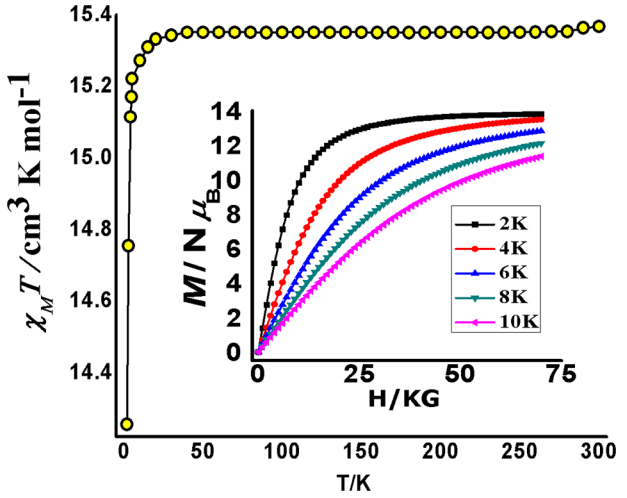

Figure 5. Temperature dependence of the DC susceptibility for complex **1** (Gd) (inset magnetization curve).

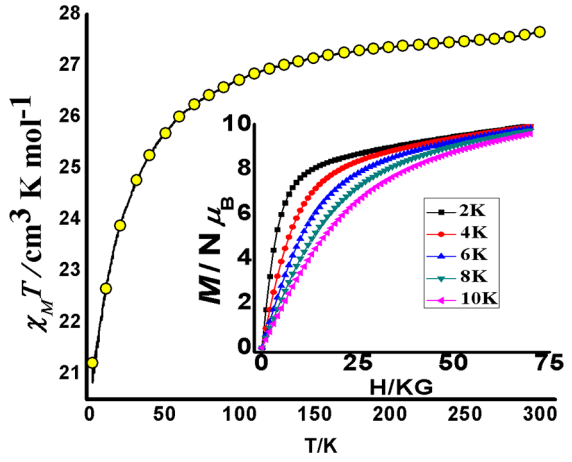

Figure 6. Temperature dependence of the DC susceptibility for complex **2** (Dy) (inset magnetization curve).

plot indicates the presence of weak antiferromagnetic interactions between the Gd^{3+} centers. With consideration of the dimeric core found in **1** (Figure S9(a) of the Supporting Information), it can be assumed that the magnetic coupling was occurring between two nearby Gd^{3+} ions through the bidentate carboxylate bridging group. The above observed antiferromagnetic coupling in complex **1** might be because of Ln···Ln separation in the dimeric unit [$Gd^{3+}\cdots Gd^{3+}$, 4.229(1) Å] and the chelating bidentate bridging mode of the carboxylate group in the dimeric unit.[28e] For complex **2**, the obtained room temperature $\chi_M T$ (χ_M = molar magnetic susceptibility) value is 27.63 cm^3 mol^{-1} K [Calculated $\chi_M T$ = 28.33 cm^3 mol^{-1} K for two uncoupled Dy^{3+} ($^6H_{15/2}$, g = 1.33)].

The molar magnetic susceptibility data of **1** and **2** were fitted according to the Curie−Weiss equation, $\chi_M = C/(T - \theta)$, which afforded the Curie constants (C) = 15.35 cm^3 mol^{-1} K for **1** and 27.63 cm^3 mol^{-1} K for **2** and Weiss constants (θ) = −0.064 K for **1** and −3.97 K for **2** (Figure S11, panels a and b, of the Supporting Information). For complex **1**, negative value of θ further confirms the presence of antiferromagnetic (AF) interaction between Gd^{3+} centers. But for complex **2**, small negative θ values do not imply the existence of antiferromagnetic interaction between Dy^{3+} centers due to the presence of large orbital angular momentum and strong spin−orbit

dx.doi.org/10.1021/cg401804e | *Cryst. Growth Des.* 2014, 14, 1287−1295

coupling for Dy^{3+}. In case of complex **2**, the $\chi_M T$ value slowly decreases down to 70 K and then decreases rapidly to a value of 20.66 $cm^3\ mol^{-1}$ K at 1.8 K, which is probably due to the thermal depopulation of excited Stark sublevels in Dy^{3+}.[29h,i,30g]Magnetization data for complex **1** was measured in the temperature range from 2 to 10 K [Figure 5 (inset)], which shows a steady increase with increasing field (**H**) and saturation values of $13.93N\mu_B$ at 7 T and 2 K, whereas for complex **2**, complete saturation was not achieved at 7 T and 2 K [Figure 6 (inset)]. The magnetization value reachs up to $10.07N\mu_B$ for **2**.

The magnetic entropy change ΔS_m for complex **1** is calculated from the magnetization data by using the Maxwell relation $\Delta S_m(T) = \int[\partial M(T,H)/\partial T]_H\ dH$.[29,30] Theoretically, the full entropy change per mole of compound corresponding to two Gd^{3+} ions is 34.58 J mol^{-1} K^{-1}, as calculated from the equation $2R\ \ln(2s + 1)$, where $s = 7/2$. So the expected value of entropy change from complex **1** will be 21.11 J kg^{-1} K^{-1}. The calculated value of $-\Delta S_m$ obtained through magnetization data is 17.25 J kg^{-1} K^{-1} at 3 K for ΔH = 7 T (Figure 7). The

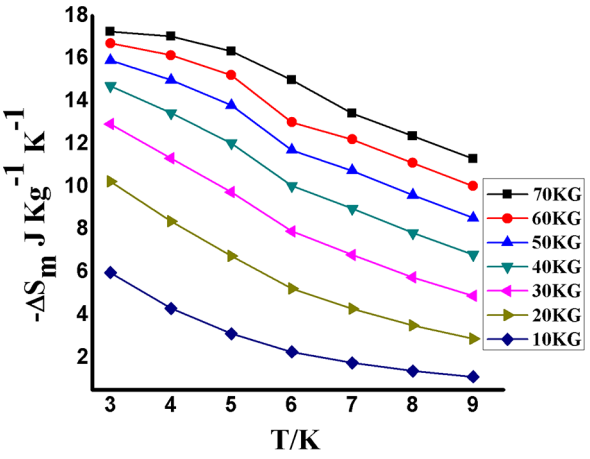

Figure 7. ΔS_m calculated by using the magnetization data of **1** at different fields and temperatures.

observed difference between the theoretical and experimental values is due to the antiferromagnetic coupling between the gadolinium centers in the dimeric unit and high M_w/N_{Gd} ratio of 818.80 (where molecular mass is M_w = 1637.61 g mol^{-1} and N_{Gd} = number of gadolinium ions present per mol of the complex **1**), indicating that complex **1** is not a dense magnetic material.

For complex **2**, the plot of $M/N\mu_B$ versus H/T (Figure S12 of the Supporting Information) shows that all isotherm magnetization curves do not collapse on the same master curve, indicating the anisotropic nature of the Dy^{3+} ions.[31] So to study the magnetic dynamics of **2**, the frequency and temperature dependencies of the alternating current (ac) susceptibilities were collected under a zero direct current (dc) field and a 3.5 G ac magnetic field (Figure S13 of the Supporting Information). The out-of-phase frequency-dependent signals below 8 K (Figure 8), indicate the onset of slow magnetic relaxation.[32]

To calculate the anisotropic energy barrier and the relaxation time, the Debye model and equation: $\ln(\chi''/\chi') = \ln(\omega\tau_0) + E_a/k_BT$ was used.[33] The best fitting results give the energy barrier $E_a/k_B \approx 17.73$ K and the relaxation time $\tau_0 \approx 9.7513 \times 10^{-7}$ s (Figure 9), which is consistent with the expected characteristic

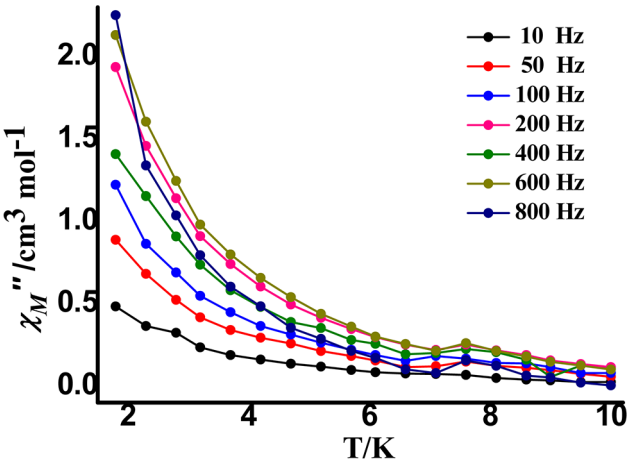

Figure 8. Temperature dependence of the out-of-phase (χ'') ac susceptibility for complex **2** at the indicated frequencies and in the zero dc field.

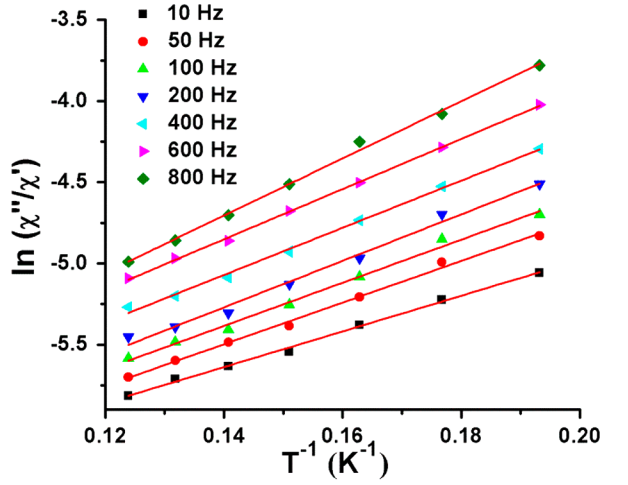

Figure 9. Plot of $\ln(\chi''/\chi')$ vs reciprocal temperature for **2**. Red solid line represents the fitting in the range of 5.2−8.1 K.

relaxation time from 10^{-6} to 10^{-11} s for SMMs.[34] The Cole−Cole or Argand plot is shown in Figure S14 of the Supporting Information, as evidence of the relaxation processes occurring in complex **2**.

Gas Adsorptions Studies. In order to evaluate the porous property, both complexes were activated under vacuum at 100 °C for 10 h. The PXRD pattern of the activated samples (Figure S2 of the Supporting Information) of both the complexes supports the stability of the framework after activation. The activated samples were introduced with different gases and solvent vapors. Adsorption analyses of **1** and **2** with N_2 show almost no uptake at 77 K. The calculated BET and Langmuir surface areas of complexes **1** and **2** from the N_2 adsorption data were 5 and 11 $m^2\ g^{-1}$ and 3.2 and 5.3 $m^2\ g^{-1}$, respectively. Considerable amount of uptake (8.4 wt % or 43.5 $cm^3\ g^{-1}$) was obtained for CO_2 gas at 195 K; this suggests the selective porous nature of the framework (Figure 10). The Henry's Law selectivity for CO_2/N_2 separation at 273 and 298 K was calculated using the equation $S_{ij} = K_H(j)/K_H(i)$ (where K_H is Henry's constant).[35] The calculated selectivity of the framework toward CO_2 over N_2 is 19 [$K_H(CO_2) = 1.4078 \times 10^{-8}$ mol g^{-1} Pa^{-1} and $K_H(N_2) = 7.2627 \times 10^{-9}$ mol g^{-1} Pa^{-1}; Table S3 of the Supporting Information). Such adsorption

dx.doi.org/10.1021/cg401804e | Cryst. Growth Des. 2014, 14, 1287−1295

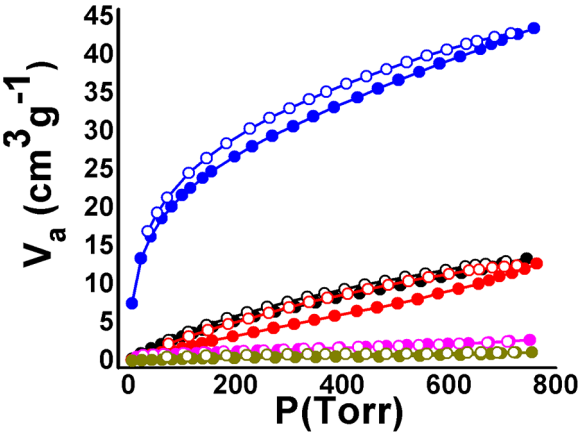

Figure 10. CO_2 and N_2 adsorption isotherm observed for complex **1**, at different temperatures (blue, 195 K; black, 273 K; and red, 298 K for CO_2 and magenta 273 K, yellow 298 K for N_2) (closed and open symbols represent adsorption and desorption branches, respectively).

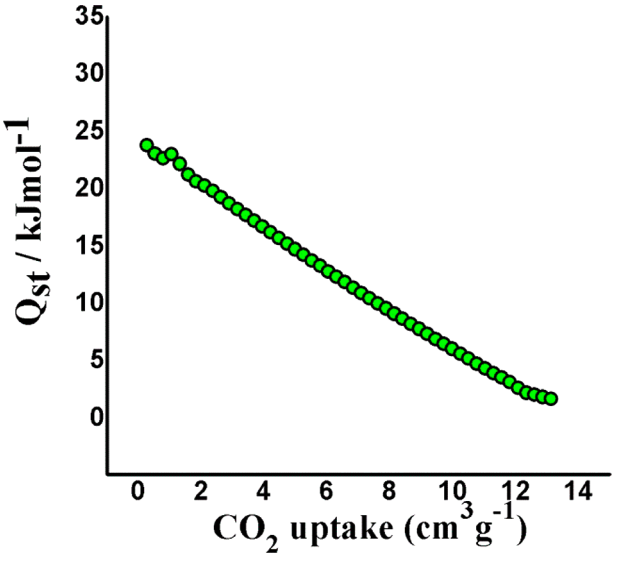

Figure 11. CO_2 isosteric heat of adsorption using adsorption data for complex **1** collected at 273 and 298 K.

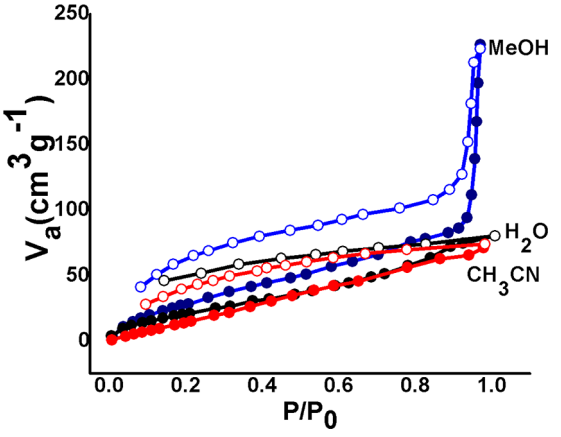

Figure 12. Solvent vapor adsorption isotherm observed for complex **1**; MeOH, (blue) H_2O (black), and CH_3CN (red) at 298 K.

selectivity of CO_2 over N_2 may be due to the fact that CO_2 molecules have a larger quadrupole moment than N_2 and has a smaller molecular size (CO_2, 3.4 Å; N_2, 3.1 Å) but bigger kinetic diameters (CO_2, 3.3 Å; N_2, 3.6 Å).[36]

Apart from this, we assume that the 3D framework, which contains Gd^{3+} ions, polar groups, and π-electrons, gives rise to an electric field that interacts with the quadrupole moment of CO_2 to provide extra stabilization energy for adsorption. This is presumably related to the hydroxyl groups of the pamoate molecules binding at the open Gd^{3+} sites and forming H bonds.[37−39] The sorption characterstics of complex **2** toward CO_2 and N_2 shows almost similar behavior as observed for complex **1** (Figure S15 of the Supporting Information). This may be due to the analogous framework structure. At 195 K, the amount of CO_2 uptake by the complex **2** is 32.2 cm^3 g^{-1} (Figure S15 of the Supporting Information). The slight difference in CO_2 uptake by complex **2** compared to complex **1** may be due to a slightly less amout of solvent accessible pore volume. The interaction of CO_2 with **1** is also reflected in the value of isosteric heat of adsorption, Q_{st} (23.79 kJ mol^{-1}), at low loading of CO_2 as calculated by the Dubinin−Radushkevich (DR) equation[40] (Figure 11). For complex **2**, the value of isosteric heat of adsorption, Q_{st}, was found around 14 kJ mol^{-1} from 298 and 273 K CO_2 adsorption isotherm data (Figure S16 of the Supporting Information).

Vapor Adsorption Studies. Solvent-vapor (H_2O, MeOH, and CH_3CN at 298 K) adsorption studies further confirms the selective polar porosity of the complexes. The activated powdered samples of both the complexes were exposed to different solvent vapors in closed vessels for 24 h. PXRD patterns of the vapor-exposed samples indicate the retention of the framework stability for both complexes (Figure S2 of the Supporting Information). The MeOH adsorption profile shows less uptake in the low-pressure region and then gradually increased up to a 0.9 P/P_o pressure, and a steep rise occurred in the isotherm. The final uptake from the profile was found to be 227 cm^3 g^{-1} for complex **1**. The lower adsorption amounts of complex **1** with other solvent vapors (CH_3CN and H_2O) further justifies the high polar nature of the pore surfaces (Figure 12). Although H_2O is more polar than MeOH, the lower adsorption amount might be due to the coordination of adsorbed water molecules to the Gd^{3+} center and the hydrogen-bonding interactions between the framework and adsorbed H_2O molecules.[41a] The PXRD pattern of the water-adsorbed sample in comparison with the as-synthesized one is further supported that water-loaded complex **1** possesses a similar structure to the as-synthesized one (Figure S2 of the Supporting Information). Due to the high polarity of methanol, it can interact effectively with the framework through different hydrogen-bonding (O−H···O/N) interactions between free −OH from pamoate and coordinated oxygen and nitrogen atoms from DMF.[41,42] This type of selectivity toward MeOH over other solvents has important implications in the separation of the mixture of solvents. Separation of MeOH over H_2O might be of more practical importance and can be employed to generate high purity MeOH. The selectivity of the framework toward MeOH vapor over CH_3CN and H_2O might be due to the well fit of MeOH molecules inside the pore, which causes stronger interactions with the MOF.[41c] Similar solvent vapor adsorption studies were also carried out for complex **2**. The results illustrate that complex **2** also shows selectivity toward methanol vapor (Figure S17). The lower uptake of methanol (201.2 cm^3 g^{-1}) for complex **2** compared to complex **1** may be due to a lower amout of solvent accessible pore volume

dx.doi.org/10.1021/cg401804e | *Cryst. Growth Des.* 2014, 14, 1287−1295

available in complex **2** compared to that of **1** (6226.5 Å^3 for complex **1** and 5766.2 Å^3 for complex **2**).

Photophysical Properties. The π-conjugated organic ligands, which usually have strongly absorbing chromophoric properties, were used effectively as sensitive reagents for tailoring lanthanide luminescence.[43] Although pamoate exhibits extended π-conjugated naphthalene moieties, the solid state photophysical properties of its lanthanide complexes are not known so far. The photoluminescence spectra of the pamoic acid and complexes **1** and **2** were measured in the solid state at room temperature (Figure 13). On excitation at 430 nm

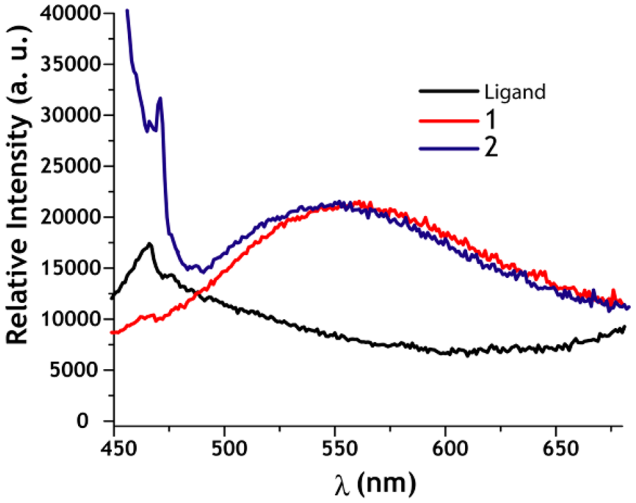

Figure 13. Solid state emission spectra of ligand pamoic acid and complexes **1** and **2** at room temperature.

(Figure S18 of the Supporting Information), complexes **1** and **2** exhibit a sharp emission peak at ~467 nm and a broad peak at ~555 nm, respectively. To get an insight into the nature of emission of complexes **1** and **2**, the emission spectra of ligand "pamoic acid" was measured. The sharp emission peak at around ~464 nm (λ_{ex} = 430 nm) was observed. The sharp emission peak at ~467 nm for **1** and **2** were similar to that of the ligand, indicating that they were attributed to the emission from the ligand. For complex **2** (Dy^{3+}), the broad emission peak observed in the region of 470−670 nm might be due to the overlap of two peaks originating from the transition $^4F_{9/2} \rightarrow {}^6H_{15/2}$ and $^4F_{9/2} \rightarrow {}^6H_{13/2}$, which corresponds to the characteristic blue emission of the Dy^{3+} ion.[44] The observed luminescence intensity of complexes **1** and **2** are similar in the 470−670 nm region, which might be due to the similar framework arrangements. So, the aforementioned photoluminescent behavior of both complexes demonstrates that they may be potential candidates for photoluminescent materials.

CONCLUSION

We have reported synthesis and characterization of two isostructural 3D lanthanide-based MOFs. We choose lanthanides as metal centers as an attempt to explore the metal-centric properties (e.g., photoluminescent and magnetic) of MOFs, in addition to the properties related to pore size and surface area. The magnetic characterization reveals that complex **1** shows cryogenic magnetic refrigeration property, whereas **2** shows slow magnetic relaxation. Complexes **1** and **2** exhibit high methanol vapor uptake and shows selectivity in sorption toward CO_2 over N_2. From the structural revelation and fluoresence property study, it can be concluded that the ligand pamoic acid provides a good metal-to-metal distance for large pore size and also behaves like a suitable chromophoric moiety (antena) for sensitization of the lanthanides. Further work with other lanthanides are under way.

ASSOCIATED CONTENT

Supporting Information

Additional data and plots on spectroscopic characterizations, magnetic, PXRD, and gas sorption studies.This material is available free of charge via the Internet at http://pubs.acs.org. CCDC 941734 and 942172 contains supplementary crystallographic data for this paper.

AUTHOR INFORMATION

Corresponding Author

*E-mail: skonar@iiserb.ac.in. Fax: +91-755-6692392. Tel: +91-755-6692339.

Notes

The authors declare no competing financial interest.

ACKNOWLEDGMENTS

S.B., S.G., and S.S. thank IISER Bhopal for the Ph.D. fellowships. H.S.J. thanks IISER Bhopal for the post-doctoral fellowship. S.K. thanks DST (Project No. SR/FT/CS-016/2010), CSIR (Project No. 01(2473)/11/EMR II), the government of India, and IISER Bhopal for generous financial and infrastructural support.

REFERENCES

(1) (a) Farha, O. K.; Eryazici, I.; Jeong, N. C.; Hauser, B. G.; Wilmer, C. E.; Sarjeant, A. A.; Snurr, R. Q.; Nguyen, S. T.; Yazaydın, A. O.; Hupp, J. T. *J. Am. Chem. Soc.* **2012**, *134*, 15016−15021. (b) Koh, K.; Wong-Foy, A. G.; Matzger, A. J. *J. Am. Chem. Soc.* **2009**, *131*, 4184−4185. (c) Furukawa, H.; Ko, N.; Go, Y. B.; Aratani, N.; Choi, S. B.; Choi, E.; Yazaydın, A. Ö.; Snurr, R. Q.; O'Keeffe, M.; Kim, J.; Yaghi, O. M. *Science* **2010**, *329*, 424−428. (d) Farha, O. K.; Yazaydın, A. O.; Eryazici, I.; Malliakas, C. D.; Hauser, B. G.; Kanatzidis, M. G.; Nguyen, S. T.; Snurr, R. Q.; Hupp, J. T. *Nat. Chem.* **2010**, *2*, 944−948.

(2) (a) Uemura, T.; Yanaia, N.; Kitagawa, S. *Chem. Soc. Rev.* **2009**, *38*, 1228−1236. (b) Kitagawa, S.; Kitaura, R.; Noro, S. *Angew. Chem., Int. Ed.* **2004**, *43*, 2334−2375. (c) Yaghi, O. M.; O'Keeffe, M.; Ockwig, N. W.; Chae, H. K.; Eddaoudi, M.; Kim, J. *Nature* **2003**, *423*, 705−714. (d) Kepert, C. J. *Chem. Commun.* **2006**, 695−700.

(3) (a) Tranchemontagne, D. J.; Mendoza-Cortes, J. L.; O'Keeffe, M.; Yaghi, O. M. *Chem. Soc. Rev.* **2009**, *38*, 1257−1283. (b) Hurd, J. A.; Vaidhyanathan, R.; Thangadurai, V.; Ratcliffe, C. I.; Moudrakovski, I. L.; Shimizu, G. K. H. *Nat. Chem.* **2009**, *1*, 705−710. (c) Farha, O. K.; Hupp, J. T. *Acc. Chem. Res.* **2010**, *43*, 1166−1175. (d) Horcajada, P.; Serre, C.; Vallet-Regí, M.; Sebban, M.; Taulelle, F.; Ferey, G. *Angew. Chem., Int. Ed.* **2006**, *45*, 5974−5978. (e) Rocca, J. D.; Liu, D.; Lin, W. *Acc. Chem. Res.* **2011**, *44*, 957−968.

(4) (a) Sakata, Y.; Furukawa, S.; Kondo, M.; Hirai, K.; Horike, N.; Takashima, Y.; Uehara, H.; Louvain, N.; Meilikhov, M.; Tsuruoka, T.; Isoda, S.; Kosaka, W.; Sakata, O.; Kitagawa, S. *Science* **2013**, *339*, 193−196. (b) Shimomura, S.; Higuchi, M.; Matsuda, R.; Yoneda, K.; Hijikata, Y.; Kubota, Y.; Mita, Y.; Kim, J.; Takata, M.; Kitagawa, S. *Nat. Chem.* **2010**, *2*, 633−637. (c) Yanai, N.; Kitayama, K.; Hijikata, Y.; Sato, H.; Matsuda, R.; Kubota, Y.; Takata, M.; Mizuno, M.; Uemura, T.; Kitagawa, S. *Nat. Mater.* **2011**, *10*, 787−793. (d) Uemura, K.; Kitagawa, S. *Chem. Soc. Rev.* **2005**, *34*, 109−119.

(5) (a) Li, H.; Eddaoudi, M.; O'Keeffe, M.; Yaghi, O. M. *Nature* **1999**, *402*, 276−279. (b) Ockwig, N.; Friedrichs, O.; O'Keefee, M.; Yaghi, O. M. *Acc. Chem. Res.* **2005**, *38*, 176−182. (c) Wang, B.; Cote,

A. P.; Furukawa, H.; O'Keeffe, M.; Yaghi, O. M. *Nature* **2008**, *453*, 207−211. (d) Deng, H.; Grunder, S.; Cordova, K. E.; Valente, C.; Furukawa, H.; Hmadeh, M.; Gandara, F.; Whalley, A. C.; Liu, Z.; Asahina, S.; Kazumori, H.; O'Keeffe, M.; Terasaki, O.; Stoddart, J. F.; Yaghi, O. M. *Science* **2012**, *336*, 1018−1023.

(6) (a) Ferey, G. *Chem. Soc. Rev.* **2008**, *37*, 191−214. (b) Mellot-Draznieks, C.; Serre, C.; Millange, F.; Dutour, J.; Surble, S.; Margiolaki, I.; Ferey, G. *Science* **2005**, *309*, 2040−2042. (c) Latroche, M.; Surble, S.; Serre, C.; Mellot-Draznieks, C.; Llewellyn, P. L.; Lee, J. H.; Chang, J. S.; Jhung, S. H.; Ferey, G. *Angew. Chem., Int. Ed.* **2006**, *45*, 8227−8231.

(7) Jeong, N. C.; Samanta, B.; Lee, C. Y.; Farha, O. K.; Hupp, J. T. *J. Am. Chem. Soc.* **2012**, *134*, 51−54.

(8) (a) Hasell, T.; Wu, X.; Jones, J. T. A.; Bacsa, J.; Steiner, A.; Mitra, T.; Trewin, A.; Adams, D. J.; Cooper, A. I. *Nat. Chem.* **2010**, *2*, 750−755. (b) Holst, J. R.; Trewin, A.; Cooper, A. I. *Nat. Chem.* **2010**, *2*, 915−920.

(9) (a) Zhao, X.; Xiao, B.; Fletcher, A. J.; Thomas, K. M.; Bradshaw, D.; Rosseinsky, M. J. *Science* **2004**, *306*, 1012−1015. (b) Swamy, S. I.; Bacsa, J.; Jones, J. T. A.; Stylianou, K. C.; Steiner, A.; Ritchie, L. K.; Hasell, T.; Gould, J. A.; Laybourn, A.; Khimyak, Y. Z.; Adams, D. J.; Rosseinsky, M. J.; Cooper, A. I. *J. Am. Chem. Soc.* **2010**, *132*, 12773−12775.

(10) (a) Park, J.; Yuan, D.; Pham, K. T.; Li, J. R.; Yakovenko, A.; Zhou, H. C. *J. Am. Chem. Soc.* **2012**, *134*, 99−102. (b) Li, J. R.; Zhou, H. C. *Nat. Chem.* **2010**, *2*, 893−898.

(11) (a) Gagnon, K. J.; Beavers, C. M.; Clearfield, A. *J. Am. Chem. Soc.* **2013**, *135*, 1252−1255. (b) Poojary, D. M.; Zhang, B.; Clearfield, A. *J. Am. Chem. Soc.* **1997**, *119*, 12550−12559. (c) Gagnon, K. J.; Perry, H. P.; Clearfield, A. *Chem. Rev.* **2012**, *112*, 1034−1054.

(12) (a) Chapman, K. W.; Halder, G. J.; Chupas, P. J. *J. Am. Chem. Soc.* **2008**, *130*, 10524−10526. (b) Chapman, K. W.; Halder, G. J.; Chupas, P. J. *J. Am. Chem. Soc.* **2009**, *131*, 17546−17547. (c) Sava, D. F.; Rodriguez, M. A.; Chapman, K. W.; Chupas, P. J.; Greathouse, J. A.; Crozier, P. S.; Nenoff, T. M. *J. Am. Chem. Soc.* **2011**, *133*, 12398−12401.

(13) (a) Li, W.; Probert, M. R.; Kosa, M.; Bennett, T. D.; Thirumurugan, A.; Burwood, R. P.; Parinello, M.; Howard, J. A. K.; Cheetham, A. K. *J. Am. Chem. Soc.* **2012**, *134*, 11940−11943. (b) Tan, J. C.; Cheetham, A. K. *Chem. Soc. Rev.* **2011**, *40*, 1059−1080. (c) Horcajada, P.; Gref, R.; Baati, T.; Allan, P. K.; Maurin, G.; Couvreur, P.; Ferey, G.; Morris, R. E.; Serre, C. *Chem. Rev.* **2012**, *112*, 1232−1268. (d) Chalati, T.; Horcajada, P.; Gref, R.; Couvreura, P.; Serre, C. *J. Mater. Chem.* **2011**, *21*, 2220−2227. (e) Vaidhyanathan, R.; Natarajan, S.; Rao, C. N. R. *Dalton Trans.* **2003**, 1459−1464. (f) Vaidhyanathan, R.; Natarajan, S.; Rao, C. N. R. *Cryst. Growth Des.* **2003**, *3*, 47−51.

(14) (a) Benelli, C.; Gatteschi, D. *Chem. Rev.* **2002**, *102*, 2369−2388. (b) Han, Y. F.; Li, X. Y.; Li, L. Q.; Ma, C. L.; Shen, Z.; Song, Y.; You, X. Z. *Inorg. Chem.* **2010**, *49*, 10781−10787. (c) Coronado, E.; Espallargas, M. *Chem. Soc. Rev.* **2013**, *42*, 1525−1539. (d) Dechambenoit, P.; Long, J. R. *Chem. Soc. Rev.* **2011**, *40*, 3249−3265. (e) Maspoch, D.; Ruiz-Molinaa, D.; Veciana, J. *Chem. Soc. Rev.* **2007**, *36*, 770−818.

(15) (a) Binnemans, K. *Chem. Rev.* **2009**, *109*, 4283−4374. (b) Rocha, J.; Carlos, L. D.; Paz, F. A. A.; Ananiasa, D. *Chem. Soc. Rev.* **2011**, *40*, 926−940. (c) Allendorf, M. D.; Bauer, C. A.; Bhakta, R. K.; Houka, R. J. T. *Chem. Soc. Rev.* **2009**, *38*, 1330−1352. (d) Carlos, L. D.; Ferreira, R. A. S.; Bermudez, V.; Lopez, B. J.; Escribano, P. *Chem. Soc. Rev.* **2011**, *40*, 536−549. (e) Li, Z. Y.; Zhu, G. S.; Guo, X. D.; Zhao, X. J.; Jin, Z.; Qiu, S. L. *Inorg. Chem.* **2007**, *46*, 5174−5178.

(16) (a) Jia, J. H.; Lin, X.; Blake, A. J.; Champness, N. R.; Hubberstey, P.; Shao, L. M.; Walker, G.; Wilson, C.; Schröder, M. *Inorg. Chem.* **2006**, *45*, 8838−8840. (b) Chandler, B. D.; Yu, J. O.; Cramb, D. T.; Shimizu, G. K. H. *Chem. Mater.* **2007**, *19*, 4467−4473.

(17) (a) Zhao, B.; Cheng, P.; Dai, Y.; Cheng, C.; Liao, D. Z.; Yan, S. P.; Jiang, Z. H.; Wang, G. L. *Angew Chem. Int. Ed.* **2003**, *42*, 934−936. (b) Zhao, B.; Cheng, P.; Chen, X. Y.; Cheng, C.; Shi, W.; Liao, D. Z.; Yan, S. P.; Jiang, Z. H. *J. Am. Chem. Soc.* **2004**, *126*, 3012−3013. (c) Zhao, B.; Chen, X. Y.; Cheng, P.; Liao, D. Z.; Yan, S. P.; Jiang, Z. H. *J. Am. Chem. Soc.* **2004**, *126*, 15394−15395. (e) Zhao, X. Q.; Zhao, B.; Ma, Y.; Shi, W.; Cheng, P.; Jiang, Z. H.; Liao, D. Z.; Yan, S. P. *Inorg. Chem.* **2007**, *46*, 5832−5834. (f) Chen, Z.; Zhao, B.; Cheng, P.; Zhao, X. Q.; Shi, W.; Song, Y. *Inorg. Chem.* **2009**, *48*, 3493−3495.

(18) (a) Du, M.; Li, C.-P.; Zhao, X.-J.; Yu, Q. *CrystEngComm* **2007**, *9*, 1011−1028. (b) Wang, S.; Yun, R.; Peng, Y.; Zhang, Q.; Lu, J.; Dou, J.; Bai, J.; Li, D.; Wang, D. *Cryst. Growth Des.* **2012**, *12*, 79−92. (c) Wang, S.; Peng, Y.; Wei, X.; Zhang, Q.; Wang, D.; Dou, J.; Lia, D.; Bai, J. *CrystEngComm* **2011**, *13*, 5313−5316. (d) Shi, X.-M.; Li, M.-X.; He, X.; Liu, H.-J.; Shao, M. *Polyhedron* **2010**, *29*, 2075−2080. (e) Wang, J.-J.; Yang, M.-L.; Hu, H.-M.; Xue, G.-L.; Li, D.-S.; Shi, Q.-Z. *Inorg. Chem. Commun.* **2007**, *10*, 269−272. (f) Shi, Q.; Sun, Y.; Sheng, L.; Ma, K.; Hu, M.; Hu, X.; Huang, S. *Cryst. Growth Des.* **2008**, *8*, 3401−3407. (g) Han, Z.-X.; Wanga, J.-J.; Hua, H.-M.; Chen, X.-L.; Wua, Q.-R.; Li, D.-S.; Shi, Q.-Z. *J. Mol. Struct.* **2008**, *891*, 364−369. (h) Li, N.; Gou, L.; Hua, H.-M.; Chen, S.-H.; Chen, X.-L.; Wang, B.-C.; Wua, Q.-R.; Yang, M.-L.; Xue, G.-L. *Inorg. Chim. Acta* **2009**, *362*, 3475−3483. (i) Baghel, G. S.; Rao, C. P. *Polyhedron* **2009**, *28*, 3507−3514.

(19) Kahn, O. *Molecular Magnetism*; Wiley-VCH: New York, 1991.

(20) Sheldrick, G. M. *SHELXTL: Program for the Solution of Crystal of Structures*; University of Göttingen: Göttingen, Germany, 1993.

(21) Sheldrick, G. M. *SHELXL 97: Program for Crystal Structure Refinement*; University of Göttingen: Göttingen, Germany, 1997.

(22) Spek, A. L. *J. Appl. Crystallogr.* **2003**, *36*, 7−13.

(23) Farrugia, L. J. *J. Appl. Crystallogr.* **1999**, *32*, 837−838.

(24) (a) Munakata, M.; Wu, L. P.; Kuroda-Sowa, T.; Maekawa, M.; Suenaga, Y.; Sugimoto, K. *Inorg. Chem.* **1997**, *36*, 4903−4905. (b) Munakata, M.; Wu, L. P.; Ning, G. L.; Kuroda-Sowa, T.; Maekawa, M.; Suenaga, Y.; Maeno, N. *J. Am. Chem. Soc.* **1999**, *121*, 4968−4976. (c) Grummt, U. W.; Birckner, E.; Klemm, E.; Egbe, D. A. M.; Heise, B. *J. Phys. Org. Chem.* **2000**, *13*, 112−126. (d) Fu, R.; Xiang, S.; Hu, S.; Wang, L.; Li, Y.; Huang, X.; Wu, X. *Chem. Commun.* **2005**, 5292−5294.

(25) Deacon, G. B.; Phillips, R. J. *Coord. Chem. Rev.* **1980**, *33*, 227−250.

(26) Spek, A. L. *PLATON: A Multipurpose Crystallographic Tool*; Utrecht University: Utrecht, The Netherlands, 2001.

(27) (a) Koberl, M.; Cokoja, M.; Herrmann, W. A.; Kuhn, F. E. *Dalton Trans.* **2011**, *40*, 6834−6859. (b) Yu, L. Q.; Huang, R. D.; Xu, Y. Q.; Liu, T. F.; Chu, W.; Hu, C. W. *Inorg. Chim. Acta* **2008**, *361*, 2115−2122. (c) Su, S.; Chen, W.; Qin, W.; Qin, C.; Song, S.; Guo, Z.; Li, G.; Song, S.; Zhu, M.; Wang, S.; Hao, S.; Zhang, H. *Cryst. Growth Des.* **2012**, *12*, 1808−1815. (d) Zhu, X.; Lu, J.; Li, X.; Gao, S.; Li, G.; Xiao, F.; Cao, R. *Cryst. Growth Des.* **2008**, *8*, 1897−1901.

(28) (a) John, D.; Urland, W. *Eur. J. Inorg. Chem.* **2006**, 3503−3509. (b) Rodhe, A.; Urland, W. *Dalton Trans.* **2006**, 2974−2978. (c) Delgado, L. C.; Fabelo, O.; Cano, J.; Pasan, J.; Delgado, F. S.; Lloret, F.; Julve, M.; Perez, C. R. *CrystEngComm* **2009**, *11*, 2131−2142. (d) Sun, Y. G.; Jiang, B.; Cui, T. F.; Xiong, G.; Smet, P. F.; Ding, F.; Gao, E. N.; Lv, T.; Eeckhout, K. V.; Poelman, D.; Verpoort, F. *Dalton Trans.* **2011**, *40*, 11581−11590. (e) Majeed, J.; Mondal, K. C.; Kostakis, G. E.; Lan, Y.; Anson, C. E.; Powell, A. K. *Chem. Commun.* **2010**, *46*, 2551−2553.

(29) (a) Colacio, E.; Ruiz, G.; Lorusso, G.; Brechin, E. K.; Evangelisti, M. *Chem. Commun.* **2013**, *49*, 3845−3847. (b) Zheng, Y. Z.; Evangelisti, M.; Winpenny, R. E. P. *Angew. Chem., Int. Ed.* **2011**, *50*, 3692−3695. (c) Langley, S. K.; Chilton, N. F.; Moubaraki, B.; Hooper, T.; Brechin, E. K.; Evangelisti, M.; Murray, K. S. *Chem. Sci.* **2011**, *2*, 1166−1169. (d) Guo, F. S.; Chen, Y. C.; Liu, J.-L.; Leng, J.-D.; Meng, Z. S.; Vrábel, P.; Orendáč, M.; Tong, M.-L. *Chem. Commun.* **2012**, *48*, 12219−12221. (e) Guo, F.-S.; Leng, J. D.; Liu, J. L.; Meng, Z. S.; Tong, M. L. *Inorg. Chem.* **2012**, *51*, 405−413. (f) Goswami, S.; Adhikary, A.; Jena, H. S.; Konar, S. *Dalton Trans.* **2013**, *42*, 9813−9817. (g) Biswas, S.; Adhikary, A.; Goswami, S.; Konar, S. *Dalton Trans.* **2013**, *42*, 13331−13334. (h) Chang, L. X; Xiong, G.; Wang, L.; Cheng, P.; Zhao, B. *Chem. Commun.* **2013**, *49*, 1055−1057. (i) Shi, P.

F.; Zheng, Y. Z.; Zhao, X. Q; Xiong, G.; Zhao, B.; Wan, F. F; Cheng, P. *Chem.—Eur. J.* **2012**, *18*, 15086−15091.
(30) (a) Hooper, T. N.; Schnack, J.; Piligkos, S.; Evangelisti, M.; Brechin, E. K. *Angew. Chem., Int. Ed.* **2012**, *51*, 4633−4636. (b) Evangelisti, M.; Brechin, E. K. *Dalton Trans.* **2010**, *39*, 4672−4676. (c) Evangelisti, M.; Luis, F.; de Jongh, L. J.; Affronte, M. *J. Mater. Chem.* **2006**, *16*, 2534−2549. (d) Sibille, R.; Mazet, T.; Malaman, B.; François, M. *Chem.−Eur. J.* **2012**, *18*, 12970−12973. (e) Zheng, Y. Z.; Evangelisti, M.; Tuna, F.; Winpenny, R. E. P. *J. Am. Chem. Soc.* **2012**, *134*, 1057−1065. (f) Karotsis, G.; Evangelisti, M.; Dalgarno, S. J.; Brechin, E. K. *Angew. Chem., Int. Ed.* **2009**, *48*, 9928−9931. (g) Hou, Y. L.; Xiong, G.; Shi, P. F.; Cheng, R. R.; Zhong, J. C.; Zhao, B. *Chem. Commun.* **2013**, *49*, 6066−6068. (h) Wu, M.; Jiang, F.; Kong, X.; Yuan, D.; Long, L.; AL-Thabaiti, S. A.; Hong, M. *Chem. Sci.* **2013**, *4*, 3104−3109.
(31) (a) Zhao, L.; Xue, S.; Tang, J. *Inorg. Chem.* **2012**, *51*, 5994−5996. (b) Gass, I. A.; Moubaraki, B.; Langley, S. K.; Batten, S. R.; Murray, K. S. *Chem. Commun.* **2012**, *48*, 2089−2091.
(32) (a) Hou, Y. L.; Xiong, G.; Shen, B.; Zhao, B.; Chen, Z.; Cui, J. Z. *Dalton Trans.* **2013**, *42*, 3587−3596. (b) Habib, F.; Lin, P. H.; Long, J.; Korobkov, I.; Wernsdorfer, W.; Murugesu, M. *J. Am. Chem. Soc.* **2011**, *133*, 8830−8833. (c) Gamer, M. T.; Lan, Y.; Roesky, P. W.; Powell, A. K.; Clerac, R. *Inorg. Chem.* **2008**, *47*, 6581−6583. (d) Ke, H. S.; Xu, G. F.; Zhao, L.; Tang, J. K.; Zhang, X. Y.; Zhang, H. J. *Chem.—Eur. J.* **2009**, *15*, 10335−10338.
(33) (a) Bartolomé, J.; Filoti, G.; Kuncser, V.; Schinteie, G.; Mereacre, V.; Anson, C. E.; Powell, A. K.; Prodius, D.; Turta, C. *Phys. Rev. B* **2009**, *80*, 014430−014446. (b) Lin, S. Y.; Xu, G. F.; Zhao, L.; Guo, Y. N.; Guo, Y.; Tang, J. K. *Dalton Trans.* **2011**, *40*, 8213−8217.
(34) (a) Lin, S.-Y.; Zhao, L.; Ke, H.; Guo, Y.-N.; Tang, J.; Guo, Y.; Dou, J. *Dalton Trans.* **2012**, *41*, 3248−3252. (b) Mishra, A.; Wernsdorfer, W.; Abboud, A. K.; Christou, G. *J. Am. Chem. Soc.* **2004**, *126*, 15648−15649.
(35) (a) Nagarkar, S. S.; Chaudhari, A. K.; Ghosh, S. K. *Inorg. Chem.* **2012**, *51*, 572−576. (b) Chen, Z.; Xiang, S.; Arman, H. D.; Mondal, J. U.; Li, P.; Zhao, D.; Chen, B. *Inorg. Chem.* **2011**, *50*, 3442−3446.
(36) (a) Liu, J.; Thallapally, P. K.; McGrail, B. P.; Brown, D. R.; Liu, J. *Chem. Soc. Rev.* **2012**, *41*, 2308−2322. (b) Cui, P.; Ma, Y. G.; Li, H. H.; Zhao, B.; Li, J. R.; Cheng, P.; Balbuena, P. B.; Zhou, H. C. *J. Am. Chem. Soc.* **2012**, *134*, 18892−18895. (c) Li, J. R.; Yu, J.; Lu, W.; Sun, L. B.; Balbuena, P. B.; Zhou, H. C. *Nat. Commun.* **2013**, DOI: 10.1038/ncomms2552. (d) Li, J. R.; Ma, Y.; McCarthy, M. C.; Sculley, J.; Yu, J.; Jeong, H. K.; Balbuena, P. B.; Zhou, H. C. *Coord. Chem. Rev.* **2011**, *255*, 1791−1823.
(37) (a) Kong, X.; Scott, E.; Ding, W.; Mason, J. A.; Long, J. R.; Reimer, J. A. *J. Am. Chem. Soc.* **2012**, *134*, 14341−14344. (b) Lin, L. C.; Kim, J.; Kong, X.; Scott, E.; McDonald, T. M.; Long, J. R.; Reimer, J. A.; Smit, B. *Angew. Chem., Int. Ed.* **2013**, *52*, 4410−4413. (c) Jayaramulu, K.; Reddy, S. K.; Hazra, A.; Balasubramanian, S.; Maji, T. K. *Inorg. Chem.* **2012**, *51*, 7103−7111. (d) Li, J. R.; Kuppler, R. J.; Zhou, H. C. *Chem. Soc. Rev.* **2009**, *38*, 1477−1504. (e) Kanoo, P.; Mostafa, G.; Matsuda, R.; Kitagawa, S.; Maji, T. K. *Chem. Commun.* **2011**, *47*, 8106−8108.
(38) (a) Sumida, K.; Rogow, D. L.; Mason, J. A.; McDonald, T. M.; Bloch, E. D.; Herm, Z. R.; Bae, T. H.; Long, J. R. *Chem. Rev.* **2012**, *112*, 724−781. (b) Park, H. J.; Suh, M. P. *Chem. Sci.* **2013**, *4*, 685−690. (c) Choi, H. S.; Suh, M. P. *Angew. Chem., Int. Ed.* **2009**, *48*, 6865−6869. (d) Kim, T. K.; Suh, M. P. *Chem. Commun.* **2011**, *47*, 4258−4260.
(39) (a) Bae, Y. S.; Farha, O. K.; Hupp, J. T.; Snurr, R. Q. J. *Mater. Chem.* **2009**, *19*, 2131−2134. (b) Wilmer, C. E.; Farha, O. K.; Bae, Y. S.; Hupp, J. T.; Snurr, R. Q. *Energy Environ. Sci.* **2012**, *5*, 9849−9856. (c) Kuppler, R. J.; Timmons, D. J.; Fang, Q.-R.; Li, J.-R.; Makal, T. A.; Young, M. D.; Yuan, D.; Zhao, D.; Zhuang, W.; Zhou, H.-C. *Coord. Chem. Rev.* **2009**, *253*, 3042−3066.
(40) Dubinin, M. M. *Chem. Rev.* **1960**, *60*, 235−241.
(41) (a) Kanoo, P.; Sambhu, R.; Maji, T. K. *Inorg. Chem.* **2011**, *50*, 400−402. (b) Li, H.; Shi, W.; Zhao, K.; Niu, Z.; Chen, X.; Cheng, P. *Chem.—Eur. J.* **2012**, *18*, 5715−5723. (c) Huang, Q.; Cai, J.; Wu, H.; He, Y.; Chen, B.; Qian, G. *J. Mater. Chem.* **2012**, *22*, 10352−10355. (d) Lin, Z.; Zou, R.; Liang, J.; Xia, W.; Xia, D.; Wang, Y.; Wang, Y.; Lin, J.; Hu, T.; Chen, Q.; Wang, X.; Zhao, Y.; Burrel, A. K. *J. Mater. Chem.* **2012**, *22*, 7813−7818. (e) Han, L.; Yan, Y.; Sun, F.; Cai, K.; Borjigin, T.; Zhao, X.; Qu, F.; Zhu, G. *Cryst. Growth Des.* **2013**, *13*, 1458−1463.
(42) (a) Maji, T. K.; Uemura, K.; Chang, H. C.; Matsuda, R.; Kitagawa, S. *Angew. Chem., Int. Ed.* **2004**, *43*, 3269−3272. (b) Ghosh, S. K.; Bureekaew, S.; Kitagawa, S. *Angew. Chem., Int. Ed.* **2008**, *47*, 3403−3406. (c) Sadakiyo, M.; Yamada, T.; Kitagawa, H. *J. Am. Chem. Soc.* **2011**, *133*, 11050−11053. (d) Wu, H.; Gong, Q.; Olson, D. H.; Li, J. *Chem. Rev.* **2012**, *112*, 836−868.
(43) (a) Yersin, H.; Vogler, A. *Photochemistry and Photophysics of Coordination Compounds*; Springer-Verlag: Berlin, 1987. (b) Xu, J. G.; Wang, Z. B. *Fluorescence Analytical Methods*; Chinese Science Publishing Company: Beijing, 2006.
(44) (a) Liu, S.-J.; Huang, Y.; Lin, Z.-J.; Lib, X.-F.; Cao, R. *RSC Adv.* **2013**, *3*, 9279−9287. (d) Jung, S. H.; Yoon, S. K.; Kim, J. S. G.; Kang, J. G. *Bull. Korean Chem. Soc.* **1992**, *13*, 650−654.